

Enhancing the durability of remote-controlled gate valves through the implementation of advanced hermetic component

Zwiększenie wytrzymałości zdalnie sterowanych zaworów suwakowych poprzez zastosowanie ulepszonego komponentu hermetycznego

Jamaladdin N. Aslanov, Khalig S. Mammadov, Niyaz A. Zeynalov, Leyla R. Ibayeva

Azerbaijan State Oil and Industry University

ABSTRACT: In this study, the hermetic elements of a remote-controlled valve were scrutinized, leading to the development of an advanced hermetic unit. The primary focus was on assessing the wear resistance of this crucial component. Through meticulous analysis and experimentation, graphs illustrating wear speed and intensity over time were constructed, revealing a substantial increase in resistance compared to existing designs. Employing a combination of detailed analysis and methodical experimentation, graphical representations delineating the evolution of wear speed and intensity over time were generated. The results underscored a notable increase in resistance when compared to prevailing designs, exemplifying the heightened efficacy of the newly devised hermetic unit, which demonstrated higher durability, crucial for effective valve operation across diverse conditions. These findings signify a significant advancement in engineering, promising enhanced reliability and extended service life for valves utilizing this innovative technology. The implications extend to various industries reliant on such valves, offering improved performance and durability. Further studies, including physical experiments for surface reinforcement, can deepen the understanding of parameters such as temperature change, velocity, pressure distribution, specific heat, thermal conductivity, and turbulence dissipation over the improved valve construction's hermetic elements. The trajectory of this research aligns with the objective of refining the design and optimizing the performance of the hermetic unit, ensuring its resilience under diverse and demanding operational environments. This comprehensive exploration not only lays the groundwork for the evolution of future advancements in valve technology but also holds the potential to substantially elevate efficiency and longevity across a wide array of industrial applications.

Key words: wear, hermetic elements, wear amount, gate valve, remote-controlled valve.

STRESZCZENIE: W ramach niniejszej pracy przeanalizowano hermetyczne elementy zdalnie sterowanego zaworu, w wyniku czego opracowano ulepszony moduł hydrauliczny. Główny nacisk położono na ocenę odporności tego kluczowego elementu na zużycie. W oparciu o szczegółową analizę i eksperymenty opracowano wykresy ilustrujące szybkość i intensywność zużycia w czasie, ujawniając znaczny wzrost odporności w porównaniu z istniejącymi konstrukcjami. Poprzez połączenie szczegółowej analizy i metodycznych eksperymentów, wygenerowano wykresy graficzne określające ewolucję prędkości i intensywności zużycia w czasie. Uzyskane wyniki wskazują na znaczny wzrost odporności w porównaniu z dotychczasowymi konstrukcjami, co świadczy o zwiększonej skuteczności nowo opracowanego modułu hermetycznego, który wykazał wyższą trwałość, kluczową dla skutecznego działania zaworu w różnych warunkach. Te odkrycia oznaczają znaczący postęp w inżynierii, który może przyczynić się do zwiększenia niezawodności i wydłużenia żywotności zaworów wykorzystujących tę innowacyjną technologię. Będzie to miało przełożenie na różne branże wykorzystujące takie zawory, zapewniając ich lepszą wydajność i trwałość. Dalsze badania, w tym eksperymenty fizyczne w zakresie wzmocnienia powierzchni, pozwolą lepiej zrozumieć parametry, takie jak zmiana temperatury, prędkość, rozkład ciśnienia, ciepło właściwe, przewodność cieplna i tłumienie turbulencji w hermetycznych komponentach ulepszonej konstrukcji zaworu. Kierunek tych badań jest zgodny z celem, jakim jest udoskonalenie konstrukcji i optymalizacja wydajności modułu hermetycznego, zapewniając jego odporność w zróżnicowanych i wymagających środowiskach operacyjnych. Ta kompleksowa eksploracja nie tylko kładzie podwaliny pod dalsze postępy w dziedzinie technologii zaworów, ale także może potencjalnie znacznie zwiększyć wydajność i żywotność w szerokim zakresie zastosowań przemysłowych.

Słowa kluczowe: zużycie, elementy hermetyczne, stopień zużycia, zawór zasuwowy, zawór zdalnie sterowany.

Introduction

One crucial element in the oil and gas industry is the valve utilized for transferring production between locations. The various components of valve design are consistently exposed to diverse static and dynamic forces. Additionally, these components experience wear due to friction and develop tears over time.

Valves used in drilling and production operations exhibit differences that lead to distinct reasons for failure in each scenario. Research indicates that identifying operational faults enables the categorization of failure reasons into three primary groups: deformation, wear and tear, and chemical-thermal damages (Linz et al., 2020).

Valves operate under varying pressure distributions, particularly in the oil and gas industry, where mechanical failures are the predominant concern. Abrasive wear, a specific type of mechanical wear, requires special attention. This form of wear is more complex compared to other types, occurring when abrasive particles land on friction surfaces. If the abrasive particles are smaller than the gap between pairs, their impact on wear is minimal. However, if the particles are larger than the gap, they follow the theory of micro-cutting, penetrating the softer metal and functioning as a cutting tool, thereby initiating the cutting of the harder metal as well. Alongside hand-controlled valves, there are also numerous remote-controlled valves in the industry that require particular attention to maintain efficiency over time (Quimby, 2007).

A significant advantage of remote-controlled valves is their automatic transmission of lubricant to the hermetic elements. Pneumatically operated ZMADP 80×70 type valves, in contrast to manually operated valves, stands out due to the presence of a moving part. Consequently, the transmission system includes a pneumatic cylinder and a paired disabled control system designed to manage the valve in the event of a pneumatic system failure.

For remotely operated pneumatically operated valves, it is essential that they open within 30 seconds of activation and close within 30 seconds of deactivation. However, one of the main drawbacks is the necessity to fully meet the straightness requirement when not fully open and the skewness requirement when closed (Aslanov, 2011).

At the same time, the reliability and longevity of these valves in sandy wells are very low. Most failures result from the collapse of the conditioning surfaces, which theoretically leads to a failure of the structural parameters of valves.

The structural parameters of linear motion-flow valves include the following:

- dimensions of the valve when assembled and disassembled;
- stresses generated in the parts and nodes of the valve, considering that the valve operates in an acid-alkaline

environment and is exposed to a mixture of gas and sand from the well;

- key technical indicators of the valve include the thermal processing of the components that make up the working parts and nodes of the valve, methods for strengthening their surfaces, and the compact arrangement of the parts within the valve.

The shape and dimensions of the working parts and nodes of the valve should be optimally chosen. In addition to performing their intended function, the selected parts and nodes must withstand the forces acting on them, evenly distribute these forces over their surfaces, and maintain their operability. The primary responsibility in this regard lies with the rubber element. Under operational conditions, surfaces are prone to destruction due to combined effects of corrosion and hydro-abrasive erosion.

The gate valve serves as a highly adaptable component within the system, facilitating the control of flow during production transfer by enabling opening and closing. However, the drawback lies in the substantial force needed for both opening and closing processes to prevent potential leakages caused by wear and tear. This requirement for significant force represents a primary disadvantage of gate valves. Additionally, the operation of these valves involves multiple turns to move the valve gate up and down, determining whether it is open or closed.

Numerous investigations conducted by different researchers aim to assess the impact of wear on the hermetic elements of valves. Wear is particularly prevalent along the valve walls, especially in areas with high fluid velocity. This elevated velocity can cause erosion, leading to partial valve opening and ultimately shortening the valve's lifespan. Vibration is another factor contributing to damage in the hermetic elements of the unit, as noted by Quimby (2007).

Chen et al. (2021) conducted a comprehensive examination of tribological analyses on various rigid bodies, focusing specifically on grooves. They utilized picosecond laser partially textured thrust bearings to assess the wear coefficient across these bodies. A comparative matrix was created to identify variations among the obtained results. Additionally, the authors proposed a novel approach involving a two-dimensional analytical model for the selected case. The results were translated into a two-dimensional system, incorporating the Reynolds equation to account for mass cavitation.

The oil and gas industry employs various valve designs, with most valve bodies traditionally made from carbon steel, though some have evolved to be manufactured from stainless steel. Kumar et al. (2020) investigated the enhancement of hardness in duplex stainless steel (DSS). DSS is engineered to comprise two phases, approximately 50% austenite and

50% ferrite, resulting in a material with improved corrosion resistance and increased surface hardness.

The reviewed literature primarily focuses on numerical or simulation-based solutions aimed at minimizing valve wear to enhance overall valve performance. Despite claims in these studies regarding reduced wear on hermetic elements, wear remains a factor that cannot be ignored across all components. Consequently, the consensus from these investigations is that while a reduction in wear factors for valve elements is anticipated, complete avoidance of wear is nearly unattainable.

The main purpose of this paper is to study the state of stress deformation in the hermetic elements of the remotely controlled ZMADP 80×70 type valve and to increase its longevity by renewing the construction of its internal components.

A study of friction in hermetic elements of remote-controlled valves

Parameters required for optimal valve design

Mechanical wear, primarily attributed to friction, is the predominant form of wear in the oil and gas industry. Friction is a crucial factor that requires careful consideration throughout the sealing process of hermetic elements. The interaction of working surfaces during friction generates significant heat. This process involves plastic deformation and the cutting of surface roughness, leading to distortion in the crystal lattice of the material within the parts. Localized heat generated at the contact surfaces reach up to 100 degrees Celsius, as noted by Aslanov (2011).

The size and shape of valve components depend on the mechanical and hydrostatic forces they are exposed to. Structural elements should be designed to perform their functional tasks efficiently and to distribute stresses evenly.

Considering that the main components of the valve are its shields and saddles, determining their shapes and sizes is a crucial aspect of the design process. The width of the surface of the saddle in sliding is determined depending on the value of the pressure that the material can withstand. For valves operating under high pressure, the width of the contact surface of the saddle typically ranges from 12 to 32 mm.

The thickness of the shield is another parameter that ensures the reliable operation of the valve. Its size is determined based on the amount of deformation caused by the working pressure when the valve is closed.

One of the main reasons for the failure of the shield-saddle pair is the change in the shape of the parts due to uneven distribution of the relative pressure in the stopper knot. This leads to inadequate initial wear and tear between the pairs. When the shield is pressed against the ring-shaped working surface

of the saddle under the pressure of the extracted well product, the circular part of the shield, which sits freely in the ring pair, bends along its radii (diameters). Consequently, the principle of equal distribution of relative pressure on the clamping contact surface of the shield-saddle pair is disrupted. This factor exacerbates corrosion processes of various nature due to the aggressiveness of the liquid and gas passing through the valve, the effect of abrasive and mechanical particles in their content, as well as inter-pair contact, reducing the reserve of the valve and causing it to fail quickly. Uneven distribution of relative pressure on the indicated working surface during the opening and closing of the valve, during the forward and backward movement of the shield, destroys the working surface and destroys the metal-metal contact surface (Aslanov et al., 2023).

For this reason, one of the issues raised is to ensure equal distribution of the relative pressure on the contact surface of the shield-saddle pair.

The theoretical solution for the jamming node of modern valves involves established deformation schemes caused by load distribution on the shield under working pressure.

It has been determined that the working principle of the valves under high pressures, cyclic loadings, aggressive environment and intensive corrosion and high pressures does not depend solely on the structural improvement of its jamming knot. Given the specific working conditions of oil-mining equipment, not all types of steel or other materials are suitable. Only some of available materials can be used for manufacturing such equipment (Aslanov, 2011).

This requires the preparation of the part as a whole with high strength or the application of surface strengthening methods.

Often, material selection during design is based on calculations or comparisons with similar cases. Various processing methods are then proposed to achieve the desired hardness of contact surfaces. Despite numerous scientific studies and experimental tests on material selection for valve parts, it remains essential to conduct laboratory, bench, and mine tests of the materials adopted for each new locking knot construction.

Our proposed design also addresses this issue, with a useful self-typing effect achieved by innovating the hermetic elements of the plug knot. This conditioning effect leads to increased longevity of the conditioner.

Depending on the method of mechanical processing, some roughness always remains on the surfaces of the parts within this stopper node. They rub against each other during operation, leading to effects based on both molecular (adhesion and corrosion) and mechanical (elastic and plastic deformations, micro shearing) factors. Therefore, correct processing of contact surfaces and careful selection of materials are crucial. Various methods are proposed to increase the wear resistance of the parts of the stopper knot of the valve (Žic et. al., 2020).

Studies on the design features and working principles of valves, as well as analysis of their working environments, have shown that locking knots in flat valves are usually operated under the influence of lubricating oils. This lubrication lightens the workload and positively impacts the wear resistance between the shield and the saddle.

The requirements for the locking node of valves can be grouped as follows:

- complete specification of the sizes and shapes of the stopper knot parts and the requirements for their surfaces;
- high resistance to corrosion processes caused by the working environment;
- resistance to wear;
- ensuring its strength, taking into account the influence of the environment;
- ease of manufacturing technology.

The results of analyzing existing valve designs, investigating their operating conditions and failure causes, studying of the causes of the jamming knot, and determining key design parameters indicate that efforts to ensure the reliability of the knot need expansion and renewal. The initial examination reveals that the uneven distribution of relative pressure in the locking node of valve design is a major factor that indicates the imperfection of the design in inter-pair coupling. Our proposed new design achieves a regular distribution of relative pressure between the pairs and incorporates a self-conditioning effect.

This uneven pressure distribution exacerbates corrosion processes of various nature due to the aggressiveness of the liquid and gas passing through the valve, the effect of abrasive and mechanical parts in their composition, as well as their inter-pair contact. This reduces the reliability of the valve and leads to rapid failure. Ultimately, this results in the deformation of the knot and the loss of the valve's functionality (Sathishkumar et al., 2016).

Addressing this issue requires not structural improvements but also a comprehensive approach to solving technical, technological, and economic issues.

The longevity and efficiency of the shutters depend largely on the equal distribution of relative pressure in the stopper knot, achieving inter-pair alignment during initial wear, selecting appropriate materials according to the working principle, facilitating the back-and-forth movement of the shield, taking into account the provision of the splicing between the shield-saddle pairs in the operating conditions. Furthermore, addressing issues related to the elimination of fretting on surfaces and the processing of jamming knots to meet modern requirements remains relevant (Mamedov et al., 2020).

Considering these factors, the following goal was set for the dissertation work.

Remotely controlled ZMADP – researching stress deformation in the clamping elements of the 80×70 type valve and increasing their longevity by renewing their design.

The process of material separation and disintegration from the surface of a solid body, as well as the accumulation of residual deformation during friction, which is detected by the gradual change of the shape and (or) dimensions of the body, is referred to as wear. At the beginning of the operational period, rapid wear of parts in the hermetic nodes is observed. The continuation of this cycle is related to the quality of the surfaces and the operating mode of the mechanism, and the working reserve of the friction node which is usually 1.5 and it is 2% of overall set for surface allowances. The processing period is followed by a steady wear phase, which determines the longevity of the joint. The 3rd phase is the period of dangerous wear, representing the limit state of the mechanism and limiting the working reserve. Changes in reliability indicators coincide with changes in wear indicators.

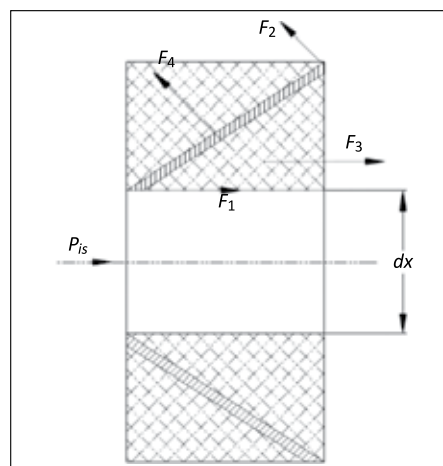


Figure 1. Structural view of new designed remote-controlled hermetic valve elements (see description below in the text)

Rysunek 1. Widok konstrukcyjny nowo zaprojektowanych zdalnie sterowanych elementów hermetycznych zaworu (opis poniżej w tekście)

Figure 1 illustrates the enhanced design of the hermetic elements within the valve structure, showing the various forces applied at different angles to these hermetic units. This design accounts for the working pressure (denoted as P_{is} [Mpa]) of the valve exerted over the nominal diameter (dx [mm]) and the body of the valve. The forces F_1 , F_2 , F_3 , F_4 , are applied independently to the hermetic elements of the valve and are distributed most proportionally across the unit (N).

The process of changing the physical and chemical properties and the geometry of the friction surface during the initial friction period is called processing. This period is characterized by stable external conditions, such as a decrease in friction force, temperature, and intensity of wear. The processing phase

involves intensive separation of material from the friction surface, significant heat release, and changes in the microgeometry of the surfaces (Dzhanakhmedov et al. 2018).

An increase in temperature at the friction boundaries causes alterations in the physical-mechanical properties of the surface layers of the material.

Experience has shown that similar unevenness always occurs after processing under different conditions and with different mating couples.

New hermetic elements calculation methodology

Calculation of new proposed element – saddle

The surface of the saddle is strengthened using a thermal-chemical method through nitriding. The contact stress on the working surface of the saddle is caused by the influence of the contact stress force on the output of the saddle surface, and it is calculated as follows (Aslanov, 2011):

$$q_{yg} = \frac{4Q_s}{\pi \cdot (D_{xy}^2 - D_1^2)} \tag{1}$$

where:

D_{xy} – outer diameter of the saddle [mm],

Q_s – the force applied to the saddle surface, representing the total contact force or load distributed over the saddle's working surface due to operational pressures [N].

The condition to ensure the smoothness of metal-metal surface and resistance to abrasion is as follows:

$$g_k \leq g_{yg} \leq g_m \tag{2}$$

where:

q_k – the minimum value of contact pressure on the working surface of the saddle that ensures tightness, determined experimentally,

q_{yg} – the relative contact pressure created by the working pressure on the outlet side of the hermetic element (in the closed condition),

q_m – the maximum value of relative contact pressure on the working surface of the hermetic element that ensures scratch resistance of working surfaces and does not impair their functionality, determined experimentally. When the above condition is satisfied, the provision of tightness is confirmed.

Calculation of new proposed element – spring

When the pressure of the working environment is $P = 0$, the initial specific pressure required on the sealing surfaces is given by:

$$q = C/\sqrt{b} \tag{3}$$

where:

C – constant quantity that takes into account the material of the spring and the saddle,

b – width of the sealing surface of the saddle [mm].

$$b = \frac{D_{s2} - D_{s1}}{2} \tag{4}$$

where:

D_{s1} – internal diameter of the spring [mm],

D_{s2} – external diameter of the saddle [mm].

The force created by spring along the axis is:

$$Q_y = \frac{4 \cdot f_0 \cdot \delta \cdot E}{x \cdot (1 - \mu^2) \cdot D_3^2} = \left[(h - f_0) \left(h - \frac{f_0}{2} \right) + \delta^2 \right] \geq Q \tag{5}$$

where:

f_0 – seat of spring,

E – modulus of elasticity of the material [N/mm²],

D_3 – external diameter of the spring [mm],

δ – thickness of the spring wall [mm],

h – height of the conical part of the bow [mm],

x – value determined from the graph,

μ – Poisson ratio,

Q – limit of the force required from the plate-shaped spring [N].

$$Q = F \cdot q \tag{6}$$

where:

F – the area of sealing surface between spring and saddle at the entrance of valve [mm²],

q – initial specific pressure [MPa].

$$F = \frac{\pi}{4} (D_2^2 - D_1^2) \tag{7}$$

Determination of axial force acting on the spindle

$$Q = Q_{sur} + Q_{kip} + Q_{sp} \tag{8}$$

where:

Q_{sur} – frictional force between saddle and spindle,

Q_{kip} – frictional force created in the hermetic elements,

Q_{sp} – force pushing spindle.

$$Q_{sur} = Q_1 + Q_2 + Q_3 \tag{9}$$

where:

Q_1 and Q_2 – frictional force at the inlet and outlet, respectively,

Q_3 – frictional force caused by pressure in the lubrication chamber.

$$Q = \pi \cdot d \cdot h \cdot P \cdot \mu_k \tag{10}$$

where:

d – diameter of spindle [mm],

h – total height of set of brackets [mm],

μ_k – coefficient of friction in hermetic elements.

Determination of diameter of the spindle thread

Internal diameter of the thread:

$$d = k \cdot \sqrt{\frac{Q_0}{[\sigma]}} + 0.3 \cdot s \tag{11}$$

where:

k – coefficient,

$[\sigma]$ – applied stress [MPa],

s – pitch of thread,

Q_0 – frictional force.

$$[\sigma] = \frac{\sigma_{ax}}{n} \tag{12}$$

where:

σ_{ax} – yield strength of the spindle material [MPa],

n – safety factor.

Results and discussion

In the course of research at the “Amirov” Oil and Gas Extraction Factory, an extensive examination was conducted to assess erosion rates in both sandy and conventional wells. The primary objective was to elucidate the complex relationships among fluid dynamics, wear, and temporal factors, resulting in distinct erosion patterns specific to each well type.

The research highlighted the pivotal role of fluid quantity in influencing wear rates in sandy and conventional wells, leading to the identification of unique wear trends (Chaiti et al., 2021). Over a comprehensive 9-month period, graphical representations were developed to illustrate the time-dependent erosion rates for each well category.

Contrary to the initial expectations of a linear increase based solely on fluid consumption, the observed trend exhibited non-linearity. Initial operational stages showed a rapid increase in consumption, followed by a steady and consistent erosion pattern after a certain period. As the operational period neared its end, there was a notable rise in re-wear, with varied manifestations in sandy and conventional wells, as shown in Figures 2 and 3.

Wear rates were quantified using a specialized formula, which provided a detailed understanding of the dynamic changes in erosion intensity over time. The results offer valuable insights into the complex interplay among fluid dynamics, temporal factors, and wear patterns in sandy and conventional wells.

These findings lay a solid foundation for developing more effective maintenance and management strategies for wells, addressing the multifaceted challenges posed by wear and erosion in the oil and gas industry.

Table 1. Duration–amount of wear dependency

Tabela 1. Zależność pomiędzy czasem a stopniem zużycia

$N\#$	t_1	t_2	t_3	t_4	t_5	t_6	t_7	t_8	t_9	t_{10}	t_{11}	t_{12}	t_{13}	t_{14}	t_{15}	t_{16}	t_{17}
t [s]	10	15	20	25	30	35	40	50	55	60	65	70	75	80	85	90	100
V_{ym} [mm]	10	15	20	25	30	35	40	50	55	60	65	70	75	80	85	90	100

$$V_y = J/t \tag{13}$$

where:

V_y – Wear Rate: This represents the rate at which material is worn away over time. It is measured in micrometers per second (m/s). Essentially, it quantifies how quickly the material is degrading or losing its volume due to wear.

J – Amount of Wear: This is the total amount of material that has been worn away. It is measured in micrometers (mic). It indicates the extent of wear that has occurred over a specific period. Amount of wear is being calculated by measuring the initial dimensions of the material, subjecting it to the wear process, and then measuring the dimensions again. The difference between the initial and final measurements gives the amount of wear.

t – Time of Wear: This is the duration over which the wear is measured. It is measured in seconds [s]. It denotes the total time during which the wear process has been observed. Time of wear records the start and end times of the wear process. The difference between these times gives the total time of wear.

V_{ym} refers to the wear amount. Since the amount of wear varies over time, a wear rate over the period of 9 months has been set. It will be shown as 1/720 as a scale. The factor 1/720 is used to normalize the wear rate on a monthly basis, where 720 represents the total number of hours in a 30-day month (30 days × 24 hours = 720 hours). By applying this scale, the wear rate is standardized for easier comparison and analysis over the specified period.

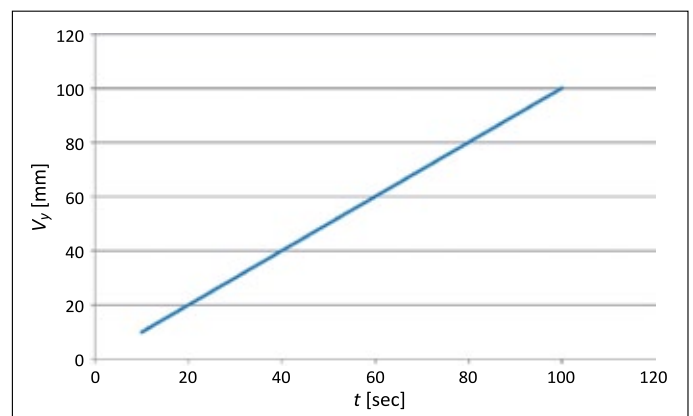


Figure 2. Duration–amount of wear dependency graph

Rysunek 2. Wykres zależności pomiędzy czasem a stopniem zużycia

Let us determine the wear rate in 9 months in conventional wells, taking into account the amount of wearing. Each month is considered to follow the previous one.

The rate of wear for 1 month:

$$V_{y1} = 0.05/1 = 0.05 \text{ mic/s}$$

The rate of wear for 2 months:

$$V_{y2} = 0.2/2 = 0.1 \text{ mic/s}$$

The rate of wear for 3 months:

$$V_{y3} = 0.36/3 = 0.12 \text{ mic/s}$$

The rate of wear for 4 months:

$$V_{y4} = 0.6/4 = 0.15 \text{ mic/s}$$

The rate of wear for 5 months:

$$V_{y5} = 0.75/5 = 0.15 \text{ mic/s}$$

The rate of wear for 6 months:

$$V_{y6} = 0.72/6 = 0.12 \text{ mic/s}$$

The rate of wear for 7 months:

$$V_{y7} = 0.7/7 = 0.1 \text{ mic/s}$$

The rate of wear for 8 months:

$$V_{y8} = 0.64/8 = 0.08 \text{ mic/s}$$

The rate of wear for 9 months:

$$V_{y9} = 0.72/9 = 0.08 \text{ mic/s}$$

Transferring the gained data to graph:

Table 2. Wear rate–time dependency table for conventional wells

Tabela 2. Tabela zależności prędkości zużycia od czasu dla odwiertów konwencjonalnych

J_y [mic]	0.05	0.20	0.36	0.60	0.75	0.72	0.70	0.64	0.72
t [s]	1	2	3	4	5	6	7	8	9
V_y [mic/s]	0.05	0.10	0.12	0.15	0.15	0.12	0.10	0.08	0.08

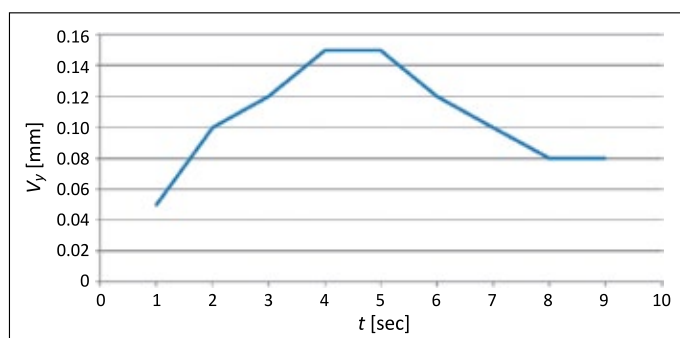


Figure 3. Wear rate–time dependency graph for conventional wells

Rysunek 3. Wykres zależności prędkości zużycia od czasu dla odwiertów konwencjonalnych

Figures 2 and 3, alongside Tables 1 and 2, provide visual insights into the dynamic evolution of wear rates over time in conventional wells. It effectively captures the undulating trend in wear rates, featuring distinct peaks and troughs. Table 2 covers each month over the period of nine months. Notably, the graph depicts the stabilization of wear rates following an

initial phase of rapid increase. Examining the finer details, during the initial time frame, the relevance of wear speed to time exhibited subtle fluctuations. Starting within the range of 0.04 to 0.06 in the early months, it gradually ascended to its peak between 0.14 and 0.16 around the 4–5 month mark. This period marks a critical phase in the operational timeline, reflecting a peak in wear intensity. Following this initial surge, a noteworthy normalization in wearing behavior became apparent. The wear rate demonstrated a discernible decline over the subsequent months. This intriguing phenomenon can be attributed to the alignment of metal-metal surfaces over time, suggesting a gradual adaptation and stabilization in the wearing process. The decrease in wear rates over time indicates a positive trend, potentially linked to improved surface compatibility and reduced friction as the operational period advances.

In essence, the comprehensive analysis of the graph not only highlights the temporal dynamics of wear rate but also unveils a valuable trend showcasing the progressive mitigation of wear effects in conventional wells. This phenomenon aligns with the hypothesis of improved surface alignment, underscoring the importance of longitudinal studies in understanding the longevity and efficiency of well components.

The wear amount–time dependency graph for conventional wells, as depicted in Figure 4 complements the insights gained from the wear rate–time dependency. This graph provides a comprehensive illustration of the cumulative effect of wear over time, offering valuable information on the overall deterioration of the well components.

Similar to the wear rate graph (Figure 3), the wear amount–time dependency graph (Figure 4) showcases intriguing trends over the operational period. In the initial months, there is a noticeable escalation in the wear amount, reflecting the cumulative impact of the higher wear speeds observed during that time. The graph effectively captures the upward trajectory of wear amount, reaching its zenith during the peak wear speed period around 4–5 months into operation. However, what distinguishes the wear amount–time dependency graph is its ability to highlight the overall decrease in wear amount as the operational period advances. This decline is indicative of a pivotal phenomenon – the adaptation and alignment of metal-metal surfaces over time. As the surfaces of the well components adjust and conform to each other, the amount of wear decreases. This aligns with the observed stabilization in wear rates and further emphasizes the significance of surface compatibility in mitigating wear effects. In summary, the wear amount–time dependency graph for conventional

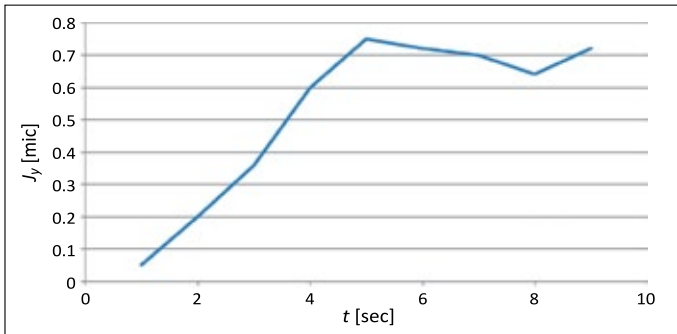


Figure 4. Wear amount–time dependency graph for conventional wells

Rysunek 4. Wykres zależności pomiędzy czasem a stopniem zużycia dla odwiertów konwencjonalnych

wells provides a holistic view of the cumulative wear impact, echoing the patterns observed in the wear rate-time dependency graph. It serves as a crucial companion, reinforcing the notion that as the operational period progresses, the alignment of metal surfaces contributes to a reduction in wear amounts, ultimately influencing the overall longevity and efficiency of conventional wells.

Let us determine the wear rate in sandy wells over the period of 9 months, taking into account the amount of wear.

The rate of wear for 1 months:

$$V_{y1} = 0.5/1 = 0.5 \text{ mic/s}$$

The rate of wear for 2 months:

$$V_{y2} = 0.12/2 = 0.6 \text{ mic/s}$$

The rate of wear for 3 months:

$$V_{y3} = 0.27/3 = 0.9 \text{ mic/s}$$

The rate of wear for 4 months:

$$V_{y4} = 0.36/4 = 0.9 \text{ mic/s}$$

The rate of wear for 5 months:

$$V_{y5} = 0.3/5 = 0.6 \text{ mic/s}$$

The rate of wear for 6 months:

$$V_{y6} = 0.36/6 = 0.6 \text{ mic/s}$$

The rate of wear for 7 months:

$$V_{y7} = 0.35/7 = 0.5 \text{ mic/s}$$

The rate of wear for 8 months:

$$V_{y8} = 0.16/8 = 0.2 \text{ mic/s}$$

The rate of wear for 9 months:

$$V_{y9} = 0.18/9 = 0.2 \text{ mic/s}$$

Let us show the obtained result in the graph:

Table 3. Wear rate–time dependency table for sandy wells

Tabela 3. Zależność prędkości zużycia od czasu dla odwiertów zapiaszczonych

V_y [mic/s]	0.5	0.6	0.9	0.9	0.6	0.6	0.5	0.2	0.2
t [s]	1	2	3	4	5	6	7	8	9
J_y [mic]	0.50	0.12	0.27	0.36	0.30	0.36	0.35	0.16	0.18

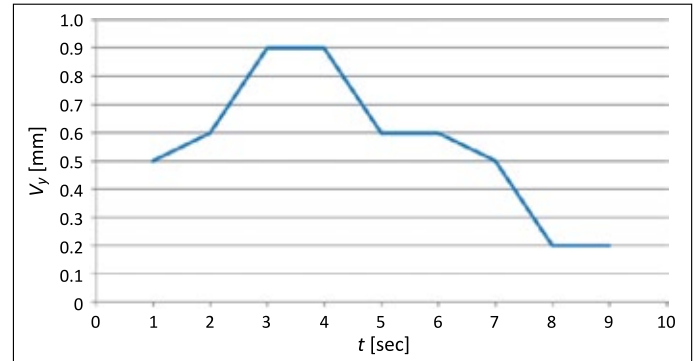


Figure 5. Wear rate–time dependency graph for sandy wells

Rysunek 5. Wykres zależności prędkości zużycia od czasu dla odwiertów zapiaszczonych

The data and accompanying graph pertaining to sandy wells offer a detailed examination of wear rate and amount over a span of 9 months. A meticulous analysis of the information reveals intriguing patterns in the erosive behavior within this specific well type. The rates of wear were meticulously calculated for each month, taking into account the varying amounts of wear. A closer inspection of the outcomes provides a nuanced perspective. In the initial month, the wear rate surged to 0.5 mic/s, initiating a phase of heightened erosive activity. The following months displayed fluctuations in wear rate, reaching a peak at 0.9 mic/s in the third month, indicating an intense erosion period. Subsequently, there was a gradual reduction in wear rate, ultimately settling at 0.2 mic/s by the ninth month.

The tabulated data in table 3 provides a systematic representation of the wear rate over the entire period. Each entry in the table serves as a snapshot of the dynamic erosive tendencies within sandy wells. The table covers each month over the nine-month timeframe

The wearing speed-time dependency graph in figure 5 visually captures the temporal evolution of wear speed. Notably, the initial spike in wear speed is succeeded by a gradual stabilization, emphasizing a potential adaptation and alignment of surfaces within the wells. The diminishing wear speed towards the end of the 9-month period hints at a possible trend of reduced erosion, suggesting an improved compatibility between the well components. In essence, the comprehensive examination of this data accentuates the intricate nature of erosive processes in sandy wells, underscoring the importance of a thorough understanding for effective well management and longevity.

Upon analysis, distinct differences emerged in the wear patterns between sandy and conventional wells, attributable to variations in the amount of fluid and subsequent wear. Graphs depicting the time-dependent erosion rates for both well types showcased linear increases in consumption over time (Figures 2 and 3). However, experimen-

tal findings revealed a nuanced dynamic, where initial rapid consumption transitioned into a more regular pattern after a specific time interval. Intriguingly, towards the end of the operational period, both well types experienced a noticeable surge in re-wearing, each manifesting distinct characteristic (Figures 4 and 5).

Focusing on the duration-amount of wear dependency, the research presented a detailed analysis of the wear rates over a 9-month period for both conventional and sandy wells. In conventional wells, the wear rate exhibited a discernible progression, with a notable increase during the initial phases of operation. However, as time advanced, the wear rate stabilized, demonstrating a consistent pattern. Towards the conclusion of the operational period, a resurgence in re-wearing was observed, showcasing a unique characteristic in conventional wells (Figure 3).

Conversely, sandy wells displayed a distinct wear pattern. The wear rate in sandy wells showcased a noticeable initial increase, followed by a more gradual progression. Notably, sandy wells demonstrated a distinct stability in wear rates, with minimal fluctuations during the latter part of the operational period. The wear rate-time dependency graph for sandy wells (Figure 5) visually captured the distinctive characteristics observed in these wells.

Conclusion

In this study, the examination of the hermetic elements within the remote-controlled valve led to the development of an innovative hermetic unit. The primary focus was on evaluating the wear resistance of this critical component. Through meticulous analysis and experimentation, graphs illustrating the wear rate and amount over time were developed, revealing a substantial increase in the wear resistance of the studied object compared to existing designs.

The newly developed hermetic unit demonstrated higher durability and longevity through systematic analysis and experimentation. The graphical representations vividly portrayed the temporal dynamics of wearing speed and intensity, highlighting the positive impact of the innovative hermetic unit. This heightened wearing resistance is crucial for ensuring prolonged and effective functioning of the remote-controlled valve across diverse operational conditions.

In conclusion, this research not only advances hermetic technology in remote-controlled valves but also substantiates tangible benefits. The heightened wear resistance observed in the studied hermetic element marks a significant stride in engineering excellence, offering improved reliability and extended service life for valves incorporating this novel technology.

These findings bear substantial implications for industries reliant on such valves, offering enhanced performance and durability in varied applications. Further studies may delve into a more detailed understanding by conducting physical experiments for surface reinforcement and investigating parameters such as temperature change, velocity, pressure distribution, specific heat, thermal conductivity, and turbulence dissipation over the improved hermetic elements of valve design.

Nomenclature

b	width of the sealing surface of the saddle [mm],
C	constant coefficient for the material of spring,
D_{s1}	internal diameter of the spring [mm],
D_{s2}	external diameter of the saddle [mm],
D_{xy}	outer diameter of the saddle [mm],
D_3	external diameter of spring [mm],
d	diameter of spindle [mm],
E	modulus of elasticity of the material [N/mm ²],
F	area of sealing [mm ²],
f_0	seat of spring,
h	height of the cone part of the bow, set of brackets [mm],
J	amount of wearing [micron],
K	coefficient,
n	safety factor,
P	pressure of working environment,
Q	limit of the force required from the plate-shaped spring [N],
Q_1	frictional force at the inlet,
Q_2	frictional force at the outlet,
Q_3	frictional force caused by pressure in the lubrication chamber,
Q_s	force applied to the saddle surface,
Q_{sur}	frictional force between saddle and spindle,
Q_{kip}	frictional force created in the hermetic elements,
Q_{sp}	force to push spindle,
q_k	minimum value of contact pressure,
q_{yg}	relative contact pressure,
q_m	maximum value of contact pressure,
s	pitch of thread,
s	second,
t	time of wearing [second],
V_y	wear rate,
x	value determined from the graph,
$[\sigma]$	yield strength [MPa],
δ	thickness of spring wall [mm],
μ	Poisson ratio.

References

Aslanov J.N., 2011. Fundamentals of Tribology. *Elm, Baku*.
 Aslanov J.N., Mammadov K.S., Zeynalov N.A., Hamidova G.A., 2023. Increasing ball valve workability by changing the design

- of its hermetic element. *International Journal on Technical and Physical Problems of Engineering*, 15(2): 214–220.
- Chaiti H., Moumen A., Jammoukh M., Mansouri K., 2021. Numerical Modeling of the Mechanical Characteristics of Polypropylene Bio-Loaded by Three Natural Fibers with the Finite Element Method. *International Journal on Technical and Physical Problems of Engineering*, 13(4): 45–50.
- Chen T., Ji J., Fu Y., Tian P., Zhou J., Yang X., 2021. Tribological analysis of picosecond laser partially textured thrust bearings with circular grooves machined: Theory and experiment. *Proceedings of the Institution of Mechanical Engineers Part J Journal of Engineering Tribology*, 208(210): 1994–1996. DOI: 10.1177/135065012111005873.
- Dzhanakhmedov A.Kh., Pirverdiev E.S., Volchenko A.I., 2018. Friction units in mechanical engineering. *Elm, Baku*.
- Kumar V.T., Prasad V.M.M., Santosh D., Prasanth C., Ranjith K., 2020. Evaluation of mechanical and interfacial properties of carbon fiber reinforced polymer (CFRP) composite materials, P.A. *College of Engineering and Technology, Pollachi*, 21(1): 477–482.
- Lin Z., Sun X., Yu T., Zhang Y., Li Y., Zhu Z., 2020. Gas–solid two-phase flow and erosion calculation of gate valve based on the CFD-DEM model. *Powder Technology*, 366(15), 395–407. DOI: 10.1016/j.powtec.2020.02.050.
- Mamedov V.T., Mamedov G.A., Aslanov J.N., 2020. Stress-Strain State of Sealing Rubber Membranes At large Deformations. *Journal of Applied Mechanics and Technical Physics*, 61(2): 286–291. DOI: 10.1134/S0021894420020157.
- Quimby B., 2007. Hydrodynamic loads. <<https://www.bgstructuralengineering.com/BGASCE7/BGASCE7006/BGASCE70604.htm>> (access: 01.03.2024).
- Sathishkumar S., Kannan M., Amirthalingam P., Arunkumar S., Natesh N.S., 2016. Material Development or Thermo Mechanical Strained Structural Application. *International Journal of Mechanical Engineering and Technology*, 7(6): 236–244.
- Žic E., Banko P., Lešnik L., 2020. Hydraulic analysis of gate valve using computational fluid dynamics (CFD). *Scientific Review Engineering and Environmental Sciences*, 29(3): 275–288. DOI: 10.22630/PNIKS.2020.29.3.23.



Jamaladdin Nuraddin ASLANOV, Ph.D.
Associate Professor at the Department of Industrial Machines
Azerbaijan State Oil and Industry University
16/21 Azadliq Ave., AZ1010 Baku, Azerbaijan
E-mail: tribo72@mail.ru



Niyaz Alimusa ZEYNALOV, M.Sc.
Doctoral student at the Department of Industrial Machines
Azerbaijan State Oil and Industry University
16/21 Azadliq Ave, AZ1010, Baku, Azerbaijan
E-mail: niyaz.zeynalov@asoiu.edu.az



Khalig Sadig MAMMADOV, M.Sc.
Doctoral student at the Department of Industrial Machines
Azerbaijan State Oil and Industry University
16/21 Azadliq Ave, AZ1010, Baku, Azerbaijan
E-mail: khalig.mammadov1993@gmail.com



Leyla Ramiz IBAYEVA, M.Sc.
Doctoral student at the Department of Industrial Machines
Azerbaijan State Oil and Industry University
16/21 Azadliq Ave, AZ1010, Baku, Azerbaijan
E-mail: ibayeva.leyla99@gmail.com